Supporting Information: Selective CVD Growth of Boron Nitride Nanotubes via Oxidation Control of Supported Catalysts

*Chunghun Kim[a‡], Yosub Kang[b,c‡], Dong Hwan Lee[a], Seung Jae Yang[c], Eunjae Jeong[d], Geunsik Lee[d] and Myung Jong Kim[a]**

[a]Department of Chemistry, Gachon University, 1342 Seongnam-daero, Sujeong-gu, Seongnam-si, Gyeonggi-do 13120, Republic of Korea. [b]R&D Center, JEIO Co., LTD, 26, MTV 5-ro, Danwon-gu, Ansan, Gyeonggi-do, Republic of Korea, [c]Department of Chemistry and Chemical Engineering, Education and Research Center for Smart Energy and Materials, Inha University, Incheon 22212, Republic of Korea. [d]Department of Chemistry, Ulsan National Institute of Science and Technology, Ulsan 44919, Republic of Korea.

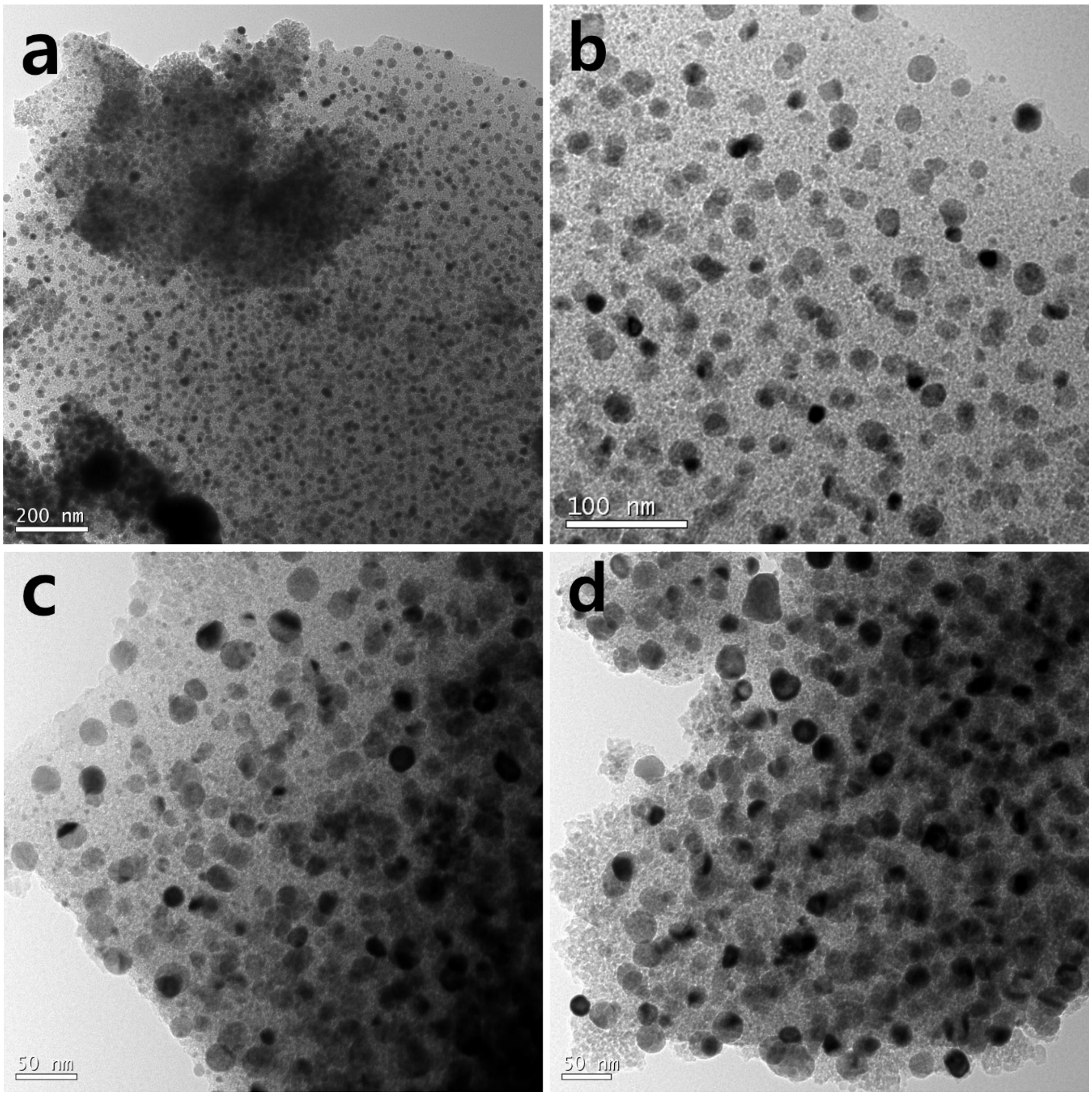

Figure S1. a~d) TEM brightfield images of synthesized Ni-Pd (MgO) catalysts.

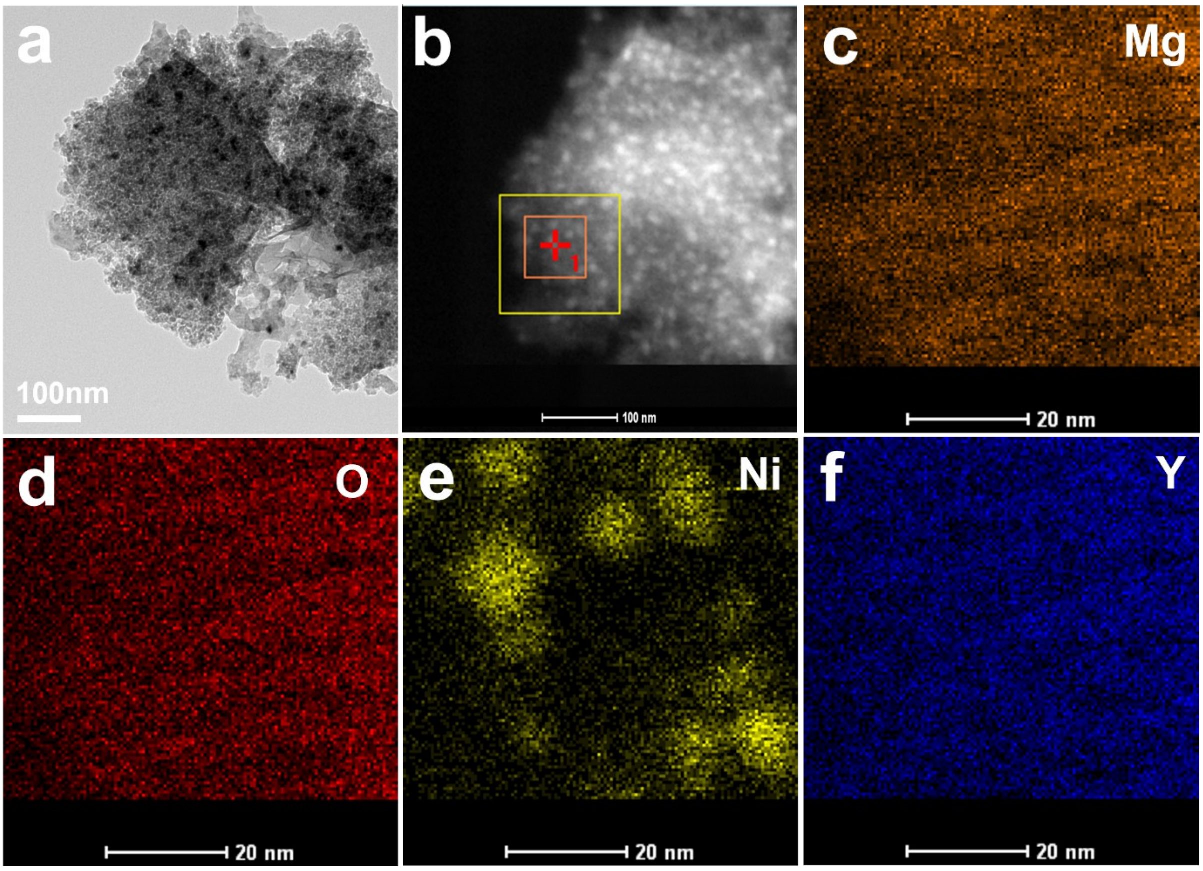

Figure S2. TEM analysis of Ni-Y catalyst supported on MgO. a) Brightfield TEM image of Ni-Y catalyst supported on MgO. b) HAADF STEM image of Ni-Y catalyst supported on MgO. c-f) EDS elemental mapping corresponding to Mg, O, Ni, and Y.

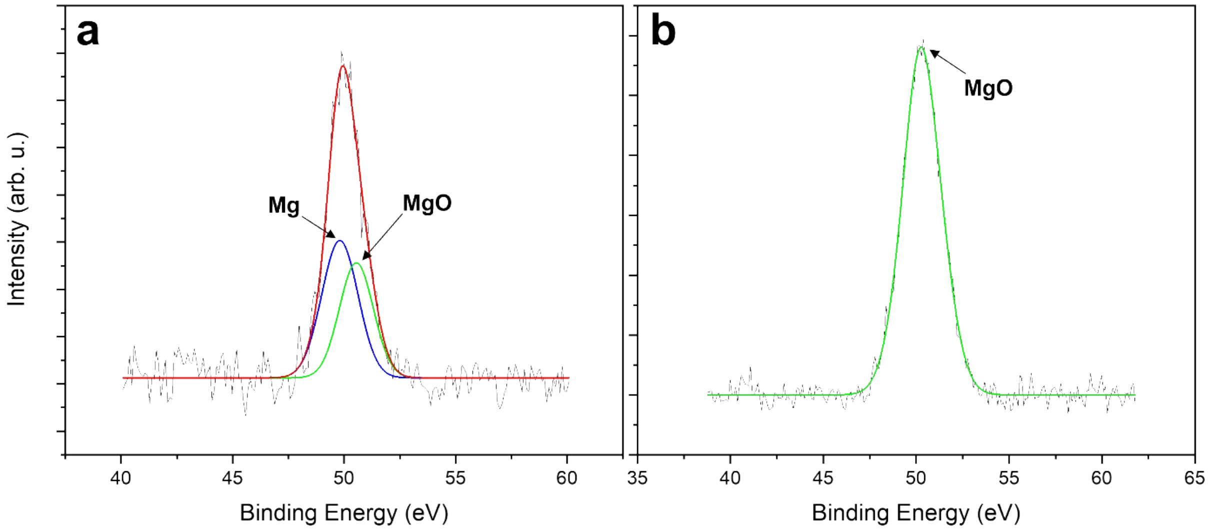

Figure S3. Mg 2p XPS spectrum of the catalyst. a) raw catalyst. b) Additional oxidized catalyst.

Table S1. Interstitial formation energies at octahedral sites, migration barriers, and BNNT-metal interfacial energies for boron and nitrogen in Fe, Co, Ni, Cu, and Pd (unit: eV). Lower (more negative) values indicate higher solubility, diffusivity, and edge preference for the corresponding element. (Data from V. Krasheninnikov et al. and J. Page et al.)

	Formation E (solubility)		Migration barrier (diffusivity)		BNNT-Metal interfacial energy (edge preference)		Crystal structure
	Boron	Nitrogen	Boron	Nitrogen	Boron	Nitrogen	
Fe	0.88	0.13	1.75	0.72	-0.95	-1.38	BCC
Co	0.62	0.55	0.97	1.25	-1.19	-1.39	HCP
Ni	0.11	0.72	1.46	1.14	-1.14	-1.21	FCC
Cu	1.51	1.97	0.86	1.05	-0.94	-1.07	FCC
Pd	-1.15	1.4	1.35	0.96	-1.14	-0.86	FCC

Table S2. Characteristic table for Ni, Pd, and Y elements.

	Atomic radius (Å)	Crystal structure	Electronegativity	Valence electron
Ni	1.35	FCC	1.91	2
Pd	1.4	FCC	2.2	4
Y	1.8	HCP	1.22	3

Figure S4. Photographs of quartz boats loaded with catalysts before and after synthesis. a) raw catalyst. b) BNNT. c) MgO-BN core/shell nanowires.

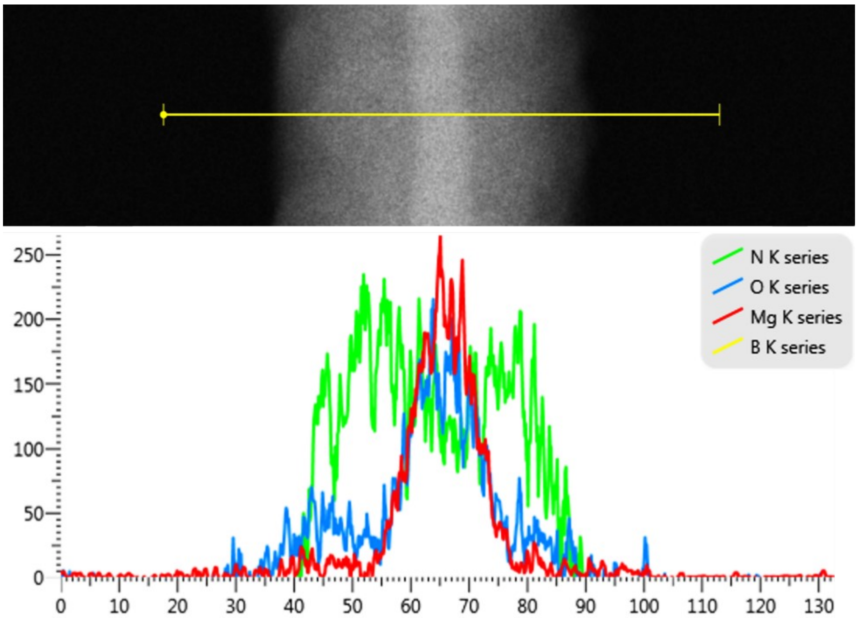

Figure S5. EDS line scan analysis of MgO-BN core/shell nanowire (Boron was not detected in this analysis because of its low cross-section for electron scattering).

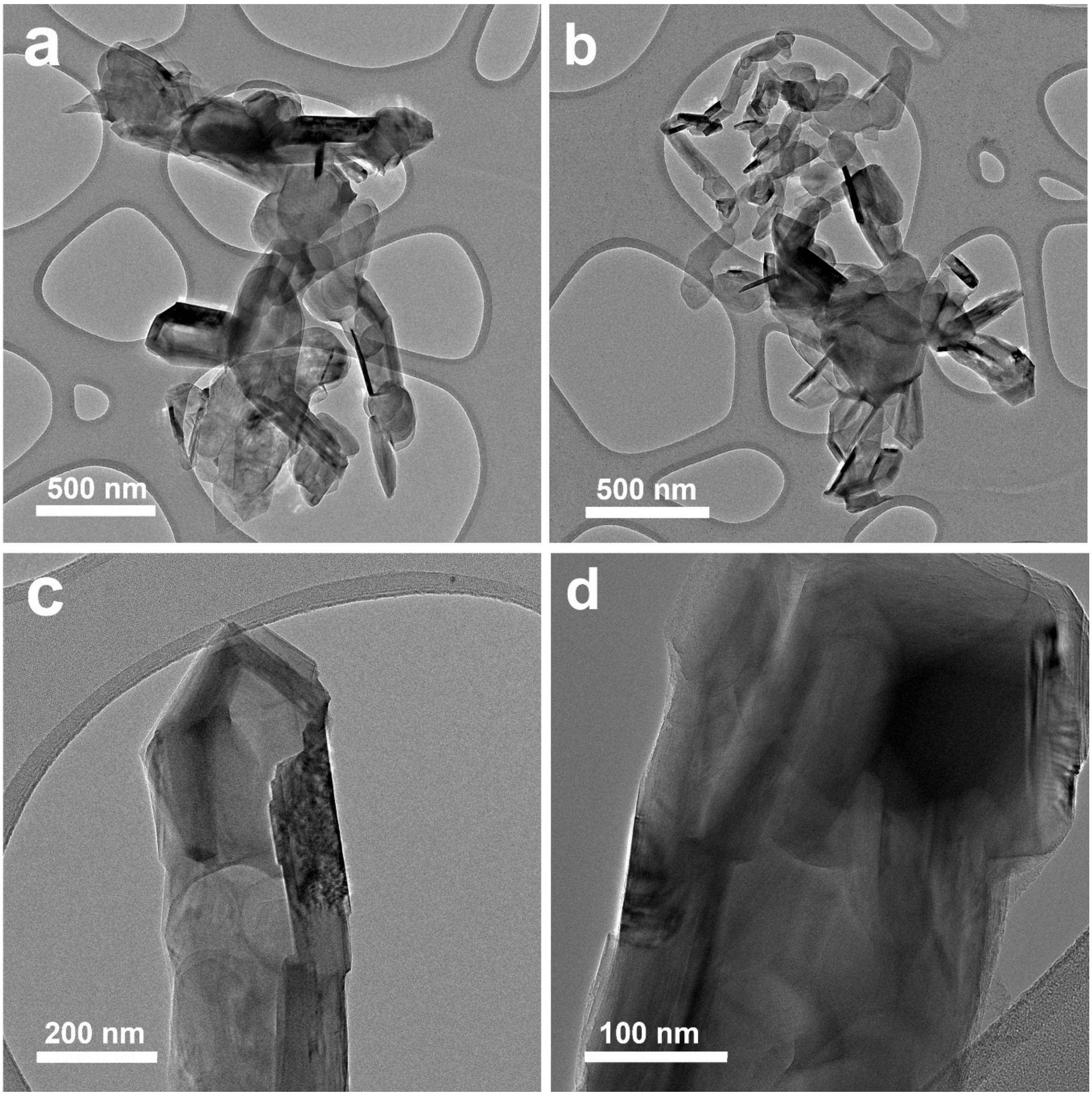

Figure S6. a-d) TEM images of BNNTs annealed at 1700℃.

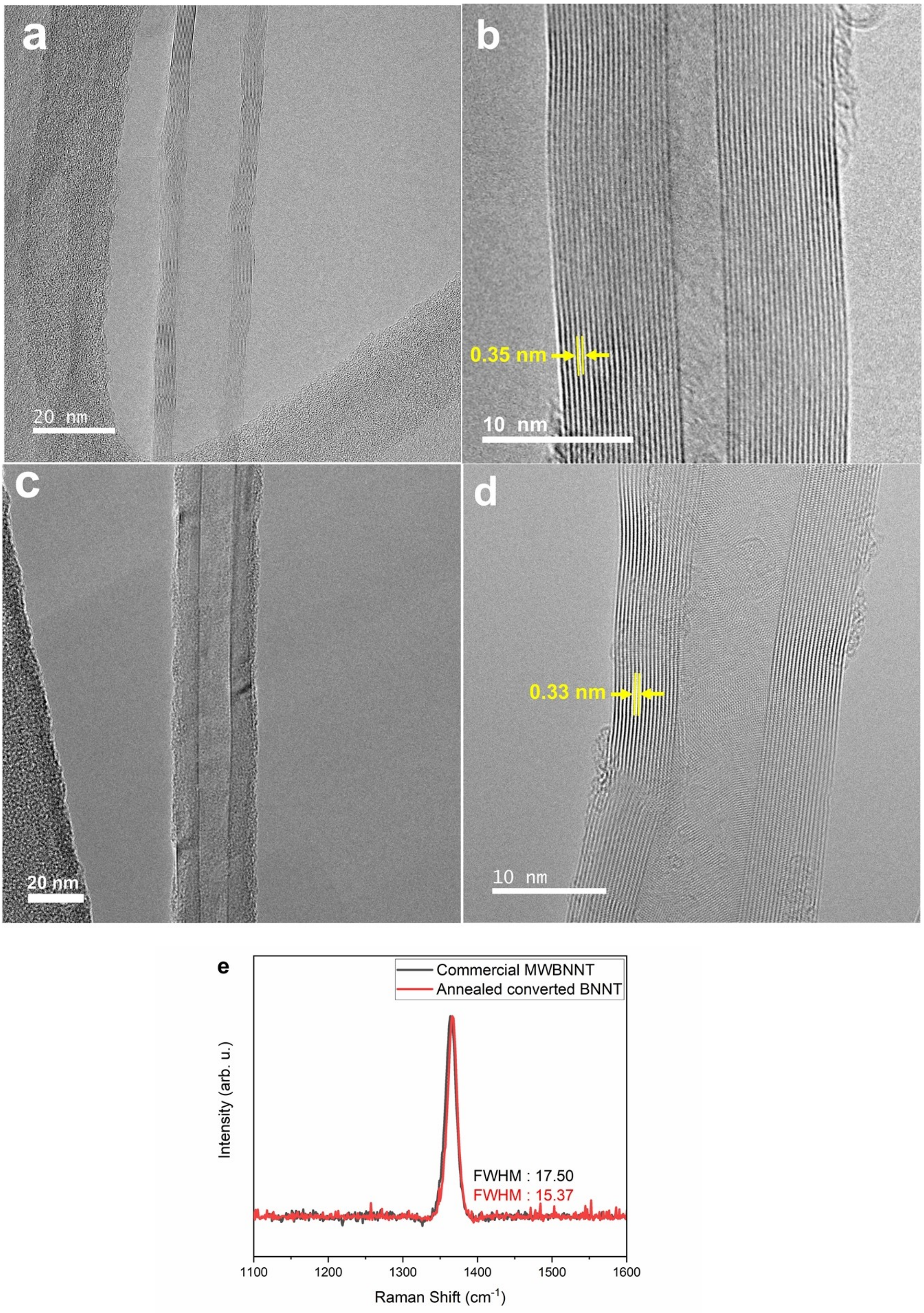

Figure S7. Comparison between converted BNNTs annealed at 1600 °C and commercially available multi-walled BNNTs (MWBNNTs). (a, b) TEM images of converted BNNTs after annealing at 1600 °C. (c, d) TEM images of commercial MWBNNTs. (e) Raman spectra of converted BNNTs annealed at 1600 °C and commercial MWBNNTs.

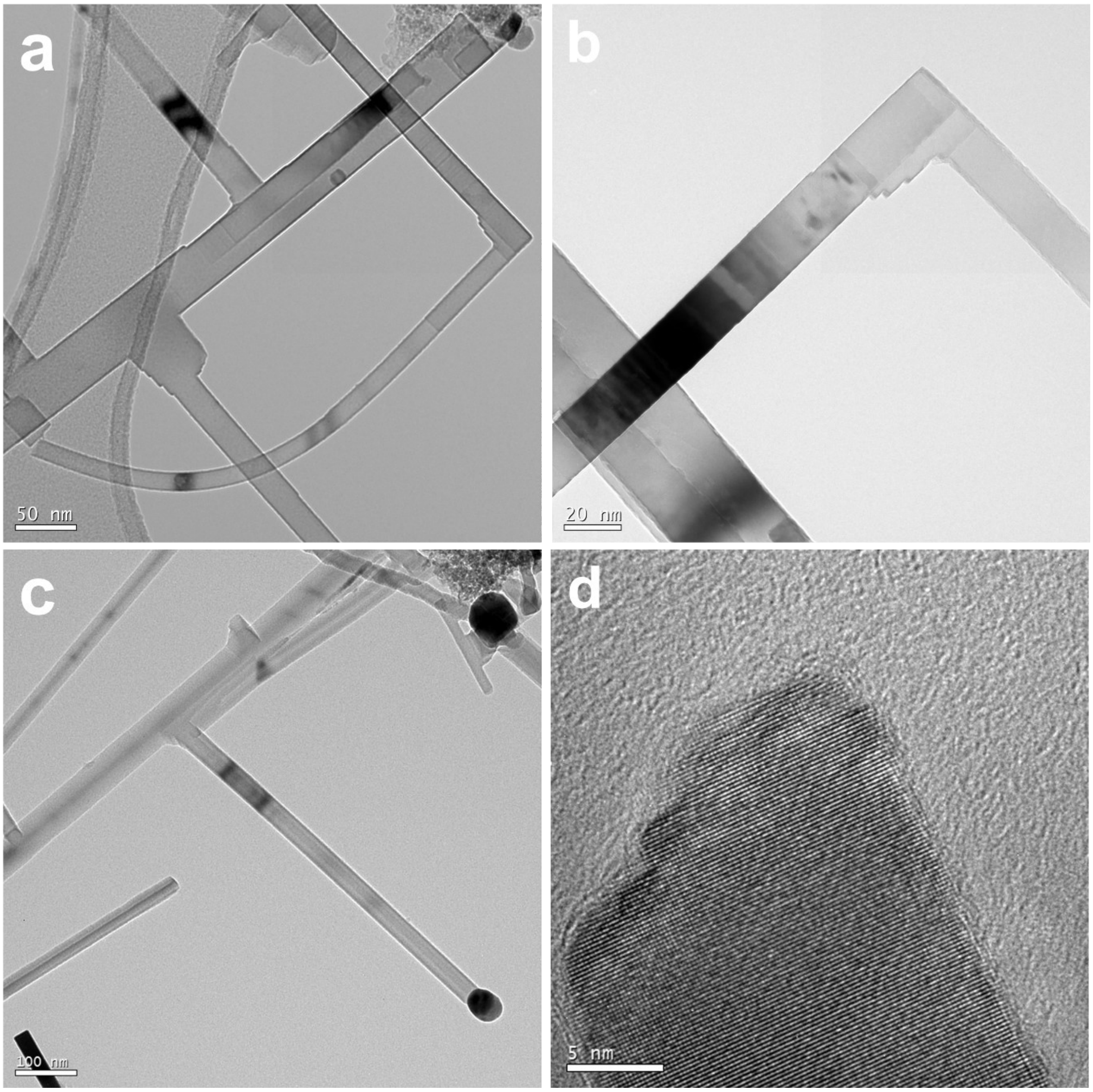

Figure S8. a,b) TEM images of MgO nanowires synthesized without BN precursors. c,d) TEM images of MgO nanowires after 1 hour BN coating at 1000℃.